IDŐJÁRÁS

Quarterly Journal of the Hungarian Meteorological Service
Vol. 118, No. 4, October – December, 2014, pp. 335–347

Some aspects of the impact of meteorological forecast uncertainties on environmental dispersion prediction

Tímea Haszpra[1*] and **András Horányi**[2]

[1]*MTA–ELTE Theoretical Physics Research Group,*
Pázmány Péter sétány 1/A, H-1117 Budapest, Hungary,
hatimi@caesar.elte.hu

[2]*Hungarian Meteorological Service,*
Kitaibel Pál u. 1., H-1024 Budapest, Hungary,
Currently on leave at the European Centre for Medium-Range Weather Forecasts,
Shinfield Park, Reading, RG2 9AX, United Kingdom
Andras.Horanyi@ecmwf.int

**Corresponding author*

(Manuscript received in final form August 25, 2014)

Abstract—There are several types of uncertainties related to the simulation of the dispersion of pollutants in the atmosphere. For a dispersion forecast, one of the most important error sources is the meteorological data produced by a numerical weather prediction model and utilized by the dispersion model. In this paper, we will present the results of an ensemble dispersion forecast created by using an ensemble meteorological forecast and the high-resolution forecast for 2.5 days. The dispersion simulations are carried out by the RePLaT Lagrangian dispersion model for particles of different radii. Significant deviations appear both in the extension and location of the ensemble of pollutant clouds consisting of particles of the same size. Differences appear also between the dispersion scenarios which use the unperturbed meteorological forecasts with different resolutions. The difference among the ensemble members increases for small particles. The area where at least one ensemble member predicts pollutant is much larger than the area covered by the pollutant cloud of the high-resolution forecast.

Key-words: dispersion, realistic particles, ensemble forecast, RePLaT model

1. Introduction

Pollutants from different sources may be advected far away from their initial position and cause pollution episodes at distant locations. The effects of ash clouds from volcano eruptions and of gases and aerosol particles from industrial accidents underline the need for investigating dispersion in the atmosphere as the emitted material can be hazardous. Volcanic ash can be dangerous, e.g., for air transport, and hence, may imply an economic hazard even if the eruption itself is not a strong one (for instance as it was the case for the Eyjafjallajökull's eruptions in 2010). The disaster of Chernobyl in 1986 and Fukushima in 2011 drew attention to the significance of the fact that radioactive materials from nuclear power plant accidents or air pollutants from other sources can also be a risk for health both in the atmosphere and as deposited material, therefore, the accurate prediction of their dispersion is essential.

As a consequence, the demand for more and more accurate tracking and forecasting of atmospheric pollutants has increased due to the growing interest in environmental problems.

However, dispersion simulations are subject to numerous uncertainties. There might be inaccuracies in the emission data for the dispersion model as the source term (the emitted amount, physical and chemical properties, emission height and period, initial extension and size distribution of the pollutant cloud) is only estimated. Obviously, in particular cases, e.g., for sudden and intense volcano eruptions, the 3-dimensional extent of the ash cloud and the size distribution of the aerosol particles can be estimated only with much more uncertainty than in other cases, like e.g., for a weak leaking from a plant close to the ground.

The other set of the input data on which the dispersion calculation is based, that is, the meteorological forecast data produced by the numerical solution of the atmospheric hydro-thermodynamic equations also include uncertainty. This is, on the one hand, the consequence of the inaccurate initial conditions of the forecasts that cannot be precisely determined due to the inaccuracies in the measurements and the approximations in the data assimilation procedures. On the other hand, the reason for the uncertainties in the meteorological data is also the fact that the meteorological weather prediction model is not fully precise as for instance it uses parameterizations for certain processes and applies numerical schemes. The uncertainty in the meteorological forecasts can be quantified by the ensemble technique including the execution of multiple meteorological forecasts (*Leutbecher* and *Palmer*, 2008). This meteorological uncertainty estimate can be carried forward to the dispersion models for assessing the implied uncertainties in the air pollution prediction.

The dispersion model itself also contains uncertainties. Its reliability depends on the processes taken into account (like advection, turbulent diffusion, dry and wet deposition, chemical reactions, etc.), their parameterizations, numerical approximations, and interpolations applied in the model. The importance of all the above-mentioned uncertainty sources is summarized in *Galmarini et al.* (2004).

Furthermore, it is important to emphasize that in 2D time-dependent flows or in 3D flows, as it is the case of the atmosphere, the advection of pollutants is chaotic. The typical characteristics of chaotic behavior are the sensitivity to the initial conditions, irregular motion, and complex but regular (fractal-like) structures (*Aref*, 1984). Thus, chaotic advection of pollutants amplifies the inaccuracies mentioned before.

It is a relevant question to understand the relative merits of the various uncertainty sources during the entire dispersion modeling process. The uncertainties related to the meteorological inputs can be minimized when such observation-related analysis meteorological fields are used as re-analysis (*Dee et al.*, 2011). With the use of re-analysis information, the meteorological inputs are considered to be perfect, therefore, only the other uncertainty sources play role in the overall uncertainty pattern of the dispersion model.

As an example, *Fig. 1* illustrates the dispersion of volcanic ash from the Eyjafjallajökull's eruption in the spring of 2010. In the beginning of the eruption period, northern flows were dominating south to Iceland, and a high pressure area was located in the Atlantic region. *Fig. 1* shows that, first, the volcanic ash becomes transported to south in the anticyclonic circulation. It is due to the northerly winds that the volcanic ash can reach even the Iberian Peninsula located about 2000 km away from Iceland. Some days later (not shown here) the volcanic ash is dispersed all over Europe. We compared the results of the simulation with satellite observation on May 10 (see right panel of *Fig. 1*). The shape of the ash cloud was found to be remarkably similar in the simulation and in the satellite image. Even the fat patch at the southwest "edge" of the ash cloud found in the simulation appears in the satellite image. Therefore, according to this comparison, there seems to be a satisfying agreement between the simulation and the measurement. This means that in this particular case, the dispersion simulation uncertainties are low, consequently, the non-meteorological related uncertainties have only a small impact. Based on this result, we consider that the uncertainties related to the meteorological inputs are presumably more important than the other ones.

Therefore, in this paper we focus on the impact of uncertainty of the meteorological forecasts on the dispersion calculation. This kind of variability was studied in different ways for gases (see, e.g., *Holt et al.*, 2009; *Lee et al.*, 2009; *Scheele* and *Sigmund*, 2001; *Straume et al.*, 1998; *Straume*, 2001). To our knowledge, no systematic investigation has been carried out for aerosol particles before the study of *Haszpra et al.* (2013). In order to study this problem we

carried out multiple dispersion simulations using 50+1 members of an ensemble forecast and the corresponding high-resolution forecast (HRES, referred as deterministic forecast in earlier references). The dispersion simulations were performed with particles of different sizes composing the pollutant clouds in order to investigate the dependence of the impact on the particle radius. This work serves as a complement to *Haszpra et al.* (2013) as the results are based on the same meteorological and emission data and, therefore, on the same dispersion simulations. Although, in contrast to that, this paper mostly concentrates on the properties of the individual pollutant clouds in the ensemble dispersion forecast rather than looking them altogether to characterize them with various statistical properties.

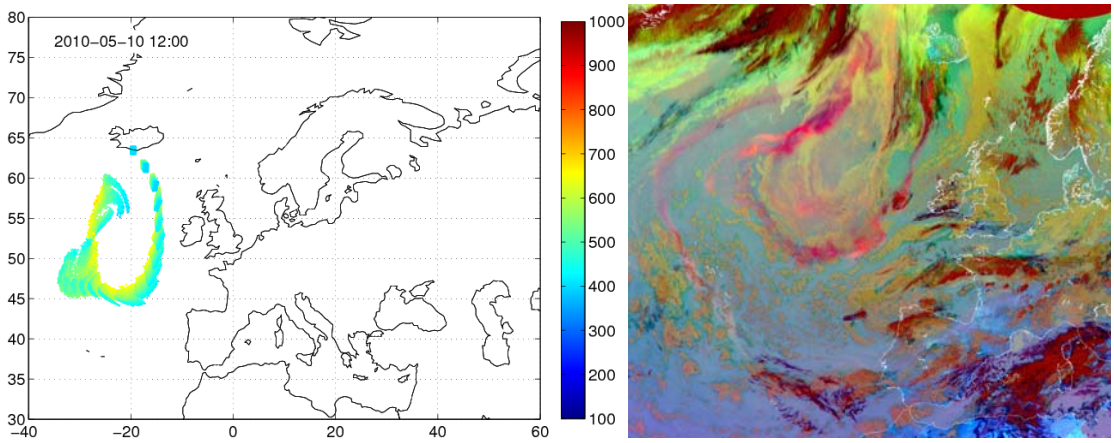

Fig. 1. Left: The dispersion of a sequence of volcanic ash puffs from the Eyjafjallajökull's eruption in RePLaT simulation (see Section 2). Each volcanic ash puff consists of 10^3 particles with radius $r = 1$ μm. The initial altitude of the centre of puffs is $p = 500$ hPa, the initial extension is 1°×1°×200 hPa. The puffs are emitted in every 6 hours from May 8, 00 UTC on. The color bar indicates the altitude of the particles in hPa. Right: Satellite image at 12 UTC, May 10, 2010. Volcanic ash is indicated by pink. [http://oiswww.eumetsat.org/WEBOPS/medialib/medialib/images/2010_05_10_1200_m8_rgb_24hmicro.jpg]

Section 2 gives a brief overview of the RePLaT dispersion model by which the dispersion simulations were carried out (it was also used for the computations shown in *Fig. 1*). In Section 3, the meteorological data utilized for the dispersion calculation is presented. Section 4 provides the results of the ensemble dispersion simulation, and Section 5 summarizes the main conclusions of the work.

2. The RePLaT dispersion model

The RePLaT (Real Particle Lagrangian Trajectory) dispersion model – as its name also suggests – is a Lagrangian trajectory model that tracks individual spherical aerosol particles with fixed, realistic radius r and density ρ_p. The velocity of a particle is equal to the velocity of the ambient air in horizontal, and in the vertical direction (owing to the impact of gravity), deposition has to be taken into account with the terminal velocity w_{term}. The effect of turbulent diffusion is built into the equations as a stochastic term. Thus, the equation of motion of a particle is the following:

$$\frac{\mathrm{d}\mathbf{r}_p}{\mathrm{d}t} = \mathbf{v} + w_{term}\mathbf{n} + \boldsymbol{\xi} \cdot \mathbf{K}, \tag{1}$$

where

$$w_{term} = -\frac{2}{9}\frac{\rho_p r^2 g}{\rho \nu}. \tag{2}$$

This follows from Stokes's law which is valid for small and heavy particles (ρ_p is in the order of 2000 kg m^{-3}, $r \leq 10$ μm). In Eq. (1) and (2), $\mathbf{r}_p(t)$ denotes the particle trajectory, $\mathbf{v} = (u, v, w)$ is the velocity of air, $\mathbf{n}$ is the vertical unit vector pointing upwards, g is gravitational acceleration, ρ and ν indicate the density and viscosity of the air, $\boldsymbol{\xi}$ is a random walk process and $\mathbf{K}$ represents the turbulent diffusivity in the different directions which might be location- and time-dependent.

RePLaT also takes into account the impact of scavenging of particles by precipitation. It is built into the model as a random process that results in a particle that is captured by a raindrop with a certain probability. The probability of the transformation from an aerosol particle to a raindrop depends on the precipitation intensity. The trajectory of the "new" particle (the particle that turned into a raindrop) is computed using the terminal velocity based on the new properties of the particle, typically using a terminal velocity w_{term} derived from the quadratic drag law for large particles:

$$w_{term} = -\frac{8}{3}\frac{\rho_{rain} r_{rain} g}{\rho C_d}, \tag{3}$$

where $C_d = 0.4$ is the drag coefficient for spheres. The transformed particle does not leave the atmosphere instantaneously, but as a raindrop falling through the air according to Eq. (1).

The meteorological data given on a grid are interpolated to the location of the particles using bicubic spline interpolation in horizontal and linear interpolation in vertical and in time. The equation of motion is solved by Euler's method. For more details about RePLaT, see *Haszpra* and *Tél* (2013).

3. Data and methods

In order to demonstrate the variability of an ensemble dispersion forecast, the RePLaT model was run with an ensemble meteorological forecast of the European Centre for Medium-Range Weather Forecasts (ECMWF) (*Molteni et al.*, 1996; *Leutbecher* and *Palmer*, 2008) including 50 perturbed members and the unperturbed control forecast (CF). Additionally, simulations were also carried out with the unperturbed high-resolution forecast (HRES). The horizontal resolution of the former ones is 0.25°×0.25°, while that of the latter is 0.125°×0.125°; the time resolution is 3 hours in both datasets. In vertical direction, the meteorological data utilized in the simulations are given on pressure levels (1000, 925, 850, 700, 500, 400, 300, 250, 200, 100, 50, 10 hPa). The dispersion calculation covers a 2.5-day period and starts at 00 UTC on March 12, 2011.

As a first approach, we are interested in the simplest case when the motion of the pollutants is determined only by advection and their terminal velocity, and the effects of turbulent diffusion and precipitation are neglected. These conditions are fulfilled in the free atmosphere with good approximation. Therefore, the simulations are carried out above the 850 hPa level (considered as the bottom of the free atmosphere), and particles sunk below this region are considered to "be deposited" and are no longer tracked.

4. Results

4.1. Ensemble evaluation of meteorological uncertainties

4.1.1. Evaluation of ensemble members

In order to study the impact of the uncertainty of the meteorological fields on the dispersion calculation, a hypothetical emission is considered centered at $\lambda = 141°$, $\varphi = 37.5°$, $p = 500$ hPa (above Japan). Initially, 9×10^4 particles of density $\rho_p = 2000$ kg m^{-3} are distributed uniformly in a horizontal square of size 1°×1°. The simulations are performed for particles of radius $r = 0$, 1, 2, …, 10 μm so that one can follow the size-dependence of the variability in the ensemble of dispersion forecast.

Particle dispersion patterns were determined in all the 50 ensemble members along with the HRES and CF members 2.5 days after the emission. However, for an easier overview, only some representative members of the whole ensemble dispersion simulation are presented here. *Fig. 2* illustrates the distribution of $r = 1$ μm aerosol particles, while *Fig. 3* is the same for $r = 4$ μm particles. The mean sea level pressure characteristics of each ensemble member are also displayed in the figures. The colors indicate the altitude of the particles

in hPa. In all dispersion simulations, the pollutant cloud of the particles is advected to east, over the Pacific Ocean. In most of them, the cloud stretches more or less in the west–east or southwest–northeast direction. This deformation is the consequence of a jet located east to Japan and some cyclones above the Pacific Ocean during these days: the strong wind shear and mixing effects related to them elongates most of the clouds (*Haszpra et al.*, 2013). The particles happen to sink in the first day. In some members, significant fraction of the $r = 1$ μm particles (having terminal velocity smaller than or of the same order as the vertical velocity component of the air) is captured by a cyclone passing towards the Californian coast. In the upwelling zone, particles lift higher in the atmosphere (green and light blue region), e.g., in members no. 6, 13, etc.

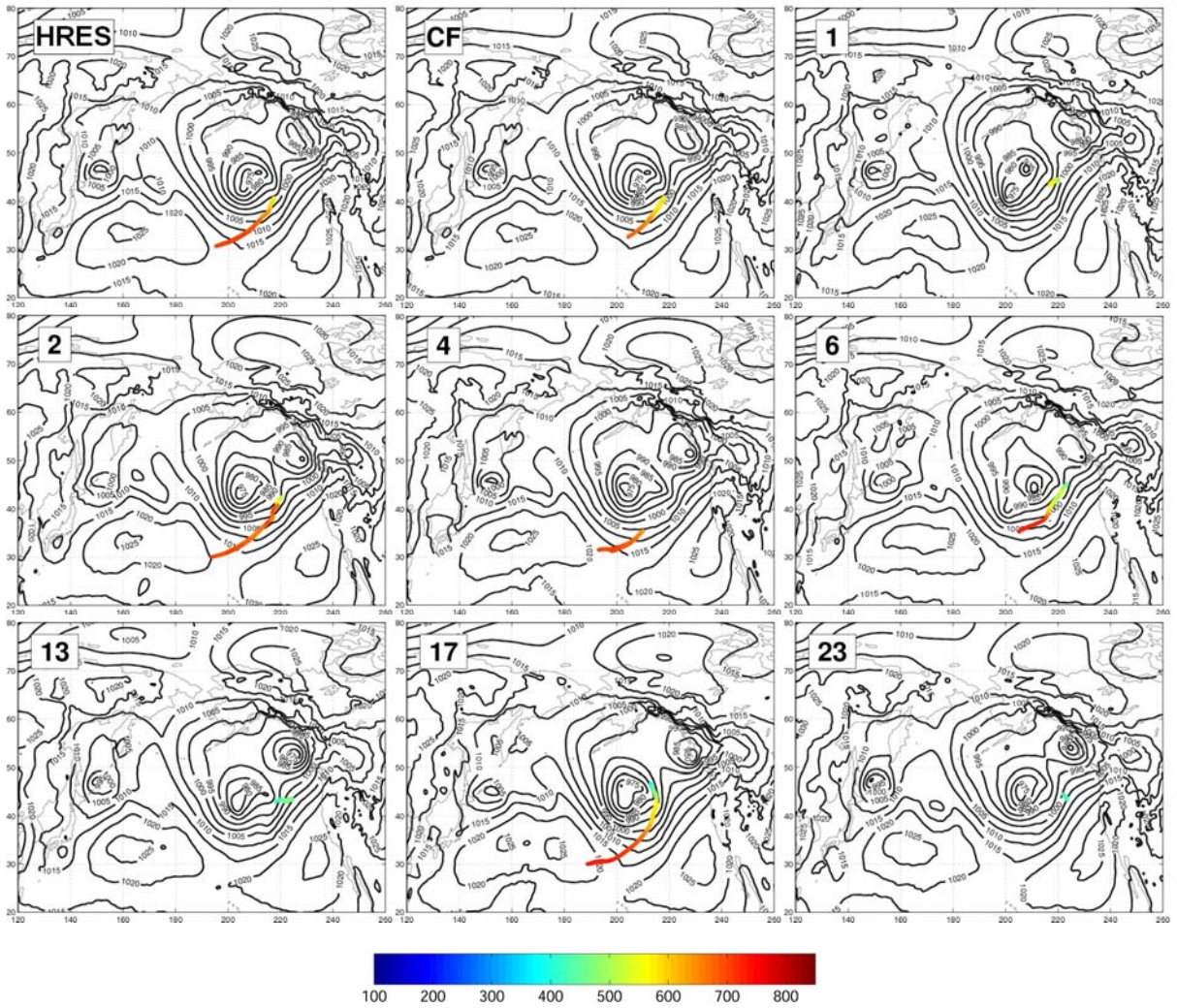

Fig. 2. The distribution of $r = 1$ μm aerosol particles 2.5 day after the emission using the high-resolution forecast (HRES), the control forecast (CF), and the perturbed ensemble members, respectively. Only some representative members of the whole ensemble dispersion simulation are presented. Color bar indicates the height of the particles in hPa. Black contours denote the mean sea level pressure in hPa.

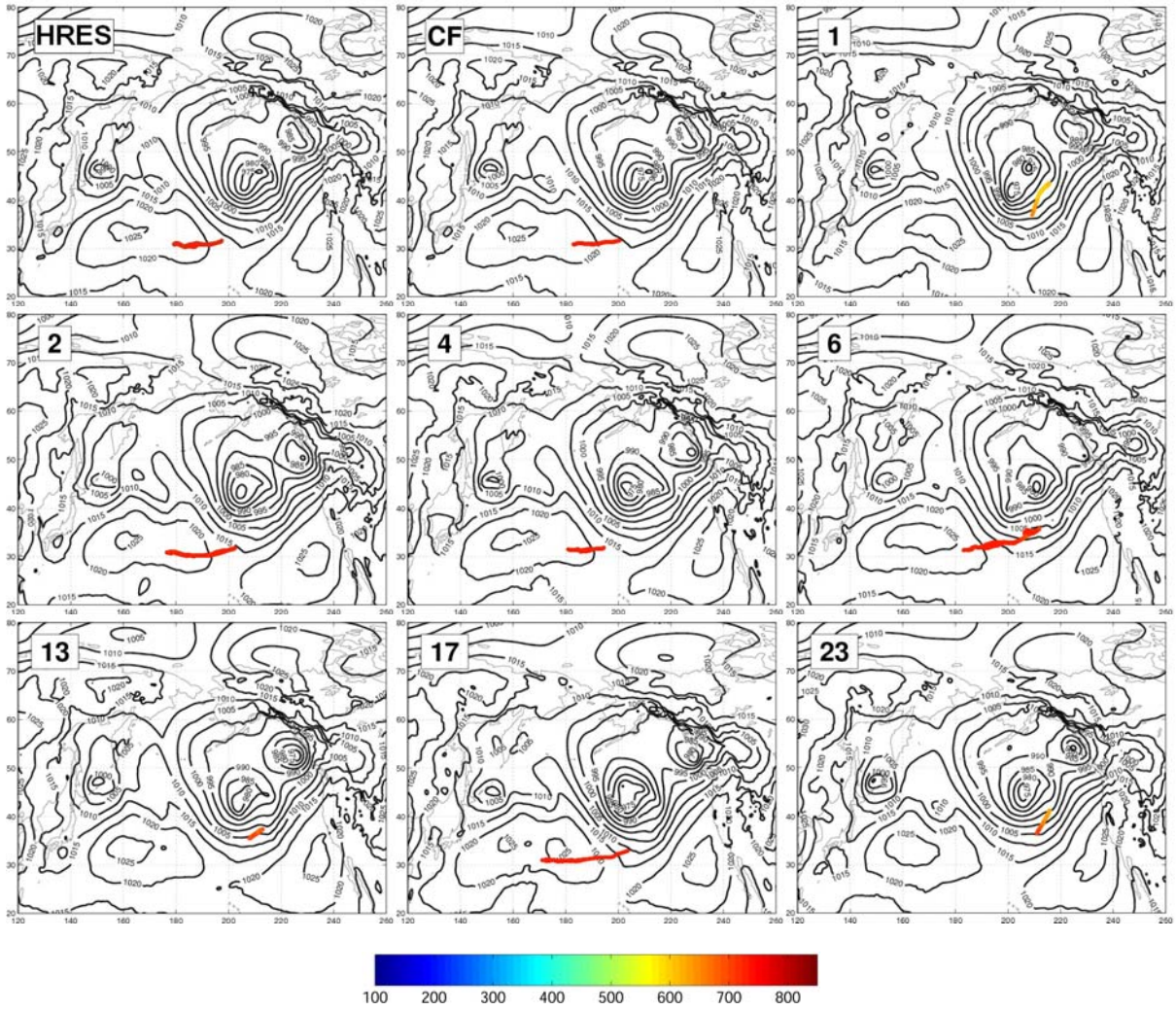

Fig. 3. The distribution of $r = 4$ μm aerosol particles 2.5 day after the emission using the high-resolution forecast (HRES), the control forecast (CF), and the perturbed ensemble members, respectively. Only some representative members of the whole ensemble dispersion simulation are presented. Color bar indicates the height of the particles in hPa. Black contours denote the mean sea level pressure in hPa.

Without any quantitative characterization of the location or extension of the pollutant clouds, just by visual inspection, different types of dispersion events can be distinguished. In *Fig. 2* for the $r = 1$ μm particles in some of the ensemble members, the pollutant cloud is hardly lengthened during the 2.5 days and remains located in the 600–350 hPa layer of the atmosphere (like no. 1, 13, 23, 43, 46[1]). Another class may be formed by dispersion members HRES and no. 2, 5, 10, 11, 14, 27, 29, etc.[1] characterized principally by orange color (750–600 hPa) and strong stretching. A similar, but distinct group can be detected e.g., from members no. 4, 20, 24, 34, 44[1] with a stretched, but less expanded shape (compared to the previous group). As mentioned before, there are

[1] Only some of the listed ensemble members are shown in *Figs. 2* and *3*.

dispersion members (e.g., no. 17, 28, 48[1]) in which the pollutant cloud is strongly influenced by the cyclonic flow, and thus, particles form a spiral towards the center of the cyclone, and the vertical extent of the pollutant cloud covers a wide region from 800 to 300 hPa (red to light blue colors). Finally, there is a similar class of members with particles lifted high in the atmosphere, where the pollutant cloud starts to turn away from the center of the western low pressure system near the North American coast due to the flow of the eastern cyclone (e.g., member no. 6, 16, 33[1]).

An analogous "visual" clustering can be carried out for the $r = 4$ μm particles based on *Fig. 3*. However, in this case fewer groups can be identified. Especially, the vertical distribution of the particles is much narrower, since these particles have 16 times greater terminal velocity than that of the $r = 1$ μm ones (based on Eq. (2)), and therefore, most of them reach the bottom level of the simulation, on which they are formally deposited, within 2.5 days. Almost all of the dispersion members can be classified into two groups: one characterized by slightly or moderately stretched shape in the west–east direction (e.g., HRES, CF, no. 2, 3, etc.[1]), and one including clouds with shorter extension and southwest–northeast direction close to the second low pressure area from North America (member no. 13, 21, 28, 46[1]). It is interesting to note that there are two "outlier" pollutant clouds in *Fig. 3* (member no. 1 and 23). Member 1 has almost all of its particles in the 750–700 hPa layer, while member 23 has half of its particles in the 800–750 hPa and 750–700 hPa layers, respectively. For both members, particles get much higher than those of the other dispersion clouds.

4.1.2. "Outlier" dispersion forecast – "outlier" meteorological forecast?

In connection with the above-mentioned "outlier" predictions for the $r = 4$ μm particles, the question arises whether dispersion member no. 1 and/or 23 is related to a strongly atypical meteorological event. The mean sea level pressure contour lines of the postage stamps charts in *Fig. 2* and *3* do not seem to confirm the idea of a likewise "outlier" meteorological forecast: the general circulation patterns of member 1 and 23 do not appear to differ much more from that of the others than the other members from each other.

Even without computing any statistical quantity, the question may be answered by comparing the $r = 1$ μm and $r = 4$ μm pollutant clouds. In the case of $r = 1$ μm particles in *Fig. 2,* both member no. 1 and no. 23 are characterized by short clouds. However, in contrast to the $r = 4$ μm particles in *Fig. 3*, they are not the only members with these properties; members no. 12, 13, 43, 46 show the same features (and possibly member 3 and 35 also can be included into the group). In the case of $r = 4$ μm particles, these members differ significantly from the two "outlier" predictions with lower and, in certain cases, longer clouds.

Based on these arguments, we cannot claim that the "outlier" members for $r = 4$ μm particles would be the consequence of considerably different meteorological forecasts. In fact, the phenomenon can be attributed to the result of the chaotic advection due to which small differences can produce significantly different dispersion patterns.

It is noted here that it would be a natural idea to run the dispersion calculations only with the representative members of the meteorological ensemble clusters in order to reduce the computational cost of the dispersion prediction. However, some studies suggest that there is not a one-to-one correspondence between the meteorological ensemble clustering and the dispersion clustering (see, e.g., *Straume*, 2001). Therefore, using only the meteorological representatives for a dispersion forecast may not necessarily give a general overview of the possible dispersion scenarios.

4.1.3. Probabilistic evaluation

It is illustrated in Section 4.1.1, that a dispersion calculation run by an ensemble meteorological forecast may result in pollutant clouds which deviate both in location and extension from each other even within 2.5 days. The difference among the pollutant clouds can be quantified by various statistical measures and probability information, see e.g. *Haszpra et al.* (2013), *Scheele* and *Sigmund* (2001), *Straume et al.* (1998), *Straume* (2001). One of the most elegant probability information is demonstrated in *Fig. 4.*

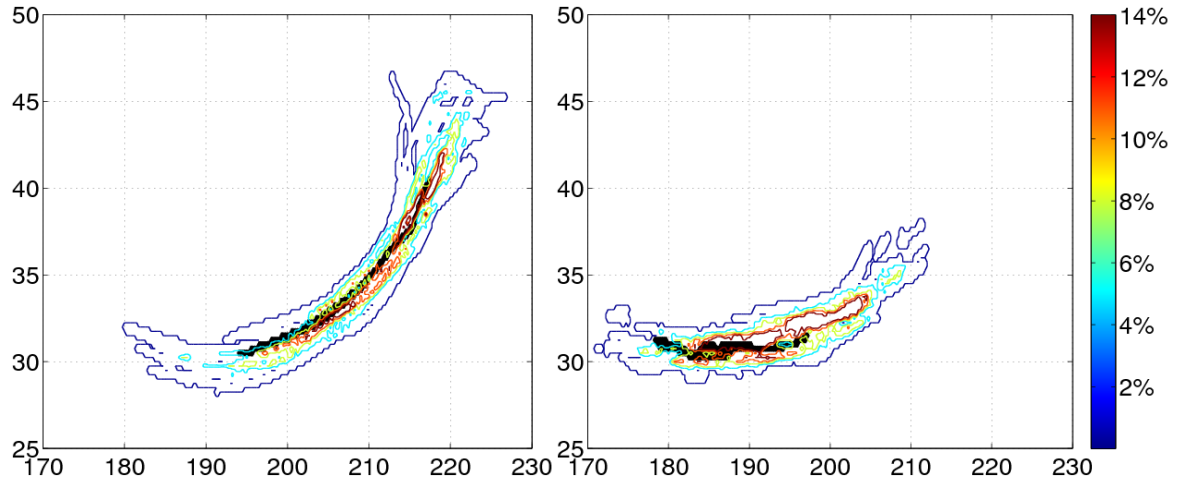

Fig. 4. Horizontal distribution of the ensemble of pollutant clouds after 2.5 days. Contours (at 2, 5, 8, 11 and 14%) indicate the percentage of the dispersion calculations predicting at least one particle in 0.25°×0.25° air columns for particles of $r = 1$ μm remained in the free atmosphere (left) and in 0.25°×0.25° cells for deposited particles of $r = 4$ μm (right). Black color denotes the pollutant cloud obtained by using the high-resolution forecast.

The particle number in 0.25°×0.25° air columns is determined for particles remained above 850 hPa, and this quantity is also calculated in 0.25°×0.25° cells in the "deposition field" for particles which subside below this level, respectively, in each member of the ensemble of pollutant clouds. The left panel of *Fig. 4* demonstrates the horizontal distribution of the ensemble of pollutant clouds in the case of $r = 1$ μm for particles remaining in the simulation range, and the right panel is the same for $r = 4$ μm for particles "deposited" within 2.5 days. Contour lines indicate areas where certain proportion of the ensemble dispersion members predicts at least one particle. Black cells demonstrate the location of the pollutant cloud given by the high-resolution forecast. Both panels of *Fig. 4* point to the fact (as expected) that the area covered by the cloud of the high-resolution forecast is much smaller than the region where at least one ensemble member predicts any particles.

This kind of information is rather useful in risk assessment when one would like to estimate the potential area in the deposition field or the region in air where the concentration of the pollutant exceeds a certain threshold.

4.2. The impact of the resolution of the meteorological data

Comparing the results of the simulations which use the unperturbed high-resolution forecast (HRES) and control forecast (CF), it is possible to study the impact of the resolution of the meteorological forecasts on the dispersion calculation. *Fig. 5* illustrates the horizontal location of the center of mass of the HRES and CF clouds for different particle radii (denoted by the numbers in μm) both for particles in the air (left) and in the deposition field (right). Neither the HRES cloud nor the CF cloud with particles of $r \geq 5$ μm have any particles in the air after 2.5 days, and similarly, clouds consisting of small particles (HRES: $r \leq 1$ μm, CF: $r \leq 2$ μm) have no particles in the deposition field.

As a general rule, it can be concluded that for all particle sizes, differences can be observed between the HRES and CF cloud centers. For those particles of the pollutant clouds that remain in the free atmosphere during the observation period (left panel), the distance between the centers of mass varies between 500 and 1400 km. In the deposition field, the distances range from about 300 km (small particles) down to the order of 10 km (large particles). This is due to the fact that larger particles have larger terminal velocities, hence they deposit sooner and the clouds have less time to separate in the different meteorological fields. *Fig. 5* reveals that also the extension of the HRES and CF pollutant cloud differs somewhat. The rate of the standard deviation values of the HRES and CF clouds in most of the cases is found to be greater than 1 (between 1.1 and 2.5). This implies that the dependence of the dispersion calculation on the resolution of the meteorological data used in the simulation is still significant, especially for pollutants consisting of small particles.

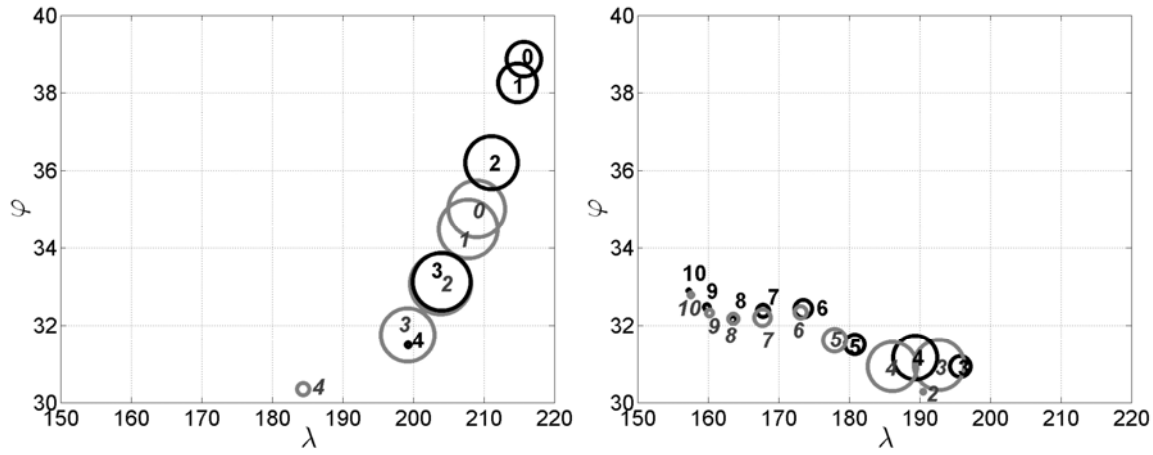

Fig. 5. The horizontal location of the center of the pollutant clouds using the high-resolution forecast (grey, italic font) and the control forecast (black, normal font). Left: center of the pollutant clouds consisting only particles remained in the air for 2.5 days. Right: the same for particles deposited during the 2.5 days. Numbers indicate the particle radius *r* of the clouds. The radii of the circles are proportional to the standard deviation of the particles within the cloud.

5. Final remarks

In this paper, the case study of a hypothetical emission illustrates that significant deviations may appear among the pollutant clouds of an ensemble of dispersion forecast, and also between the simulations using unperturbed forecasts with different resolutions, even in the simplest case when only advection influences the dispersion of the pollutants. Presumably, in simulations that take into account the impact of turbulent diffusion and precipitation on the particles, even more remarkable differences could be found, since in that case the uncertainties in the dispersion model would be enhanced.

In practice, dispersion models are usually run by a single forecast which is considered to be the best one (i.e., the high-resolution forecast). However, as the paper demonstrates, it can be useful to perform simulations using a whole ensemble of forecasts, i.e., producing an ensemble dispersion prediction in order to get a detailed and more reliable overview of the uncertainties and possible hazards related to the dispersion event.

***Acknowledgements*:** The authors thank *T. Tél* for useful suggestions. This work was partially supported by the European Union and the European Social Fund through the project FuturICT.hu (grant no. TAMOP-4.2.2.C-11/1/KONV-2012-0013), and by the Hungarian Science Foundation (grant no. OTKA NK100296).

References

Aref, H., 1984: Stirring by chaotic advection. *J. Fluid. Mech. 143*, 1–21.

Dee, D.P., Uppala, S.M., Simmons, A.J., Berrisford, P., Poli, P., Kobayashi, S., Andrae, U., Balmaseda M. A., Balsamo, G., Bauer, P., Bechtold, P., Beljaars, A.C.M., van de Berg, L., Bidlot, J., Bormann N., Delsol, C., Dragani, R., Fuentes, M., Geer, A. J., Haimberger, L., Healy, S.B., Hersbach, H., Hólm, E.V., Isaksen, L., Kållberg, P., Köhler, M., Matricardi, M., McNally, A.P., Monge-Sanz, B.M., Morcrette, J.-J., Park, B.-K., Peubey, C., de Rosnay, P., Tavolato, C., Thépaut, J.-N., Vitart, F., 2011: The ERA-Interim reanalysis: Configuration and performance of the data assimilation system. *Q. J. Roy. Meteor. Soc. 137(656)*, 553–597.

Galmarini, S., Bianconi, R., Klug, W., Mikkelsen, T., Addis, R., Andronopoulos, S., Astrup, P., Baklanov, A*., Bartniki, J., Bartzis, J., Bellasio, R., Bompay, F., Buckley, R., Bouzom, M., Champion, H., D'Amours, R., Davakis, E., Eleveld, H., Geertsema, G., Glaab, H., Kollax, M., Ilvonen, M., Manning, A., Pechinger, U., Persson, C., Polreich, E., Potemski, S., Prodanova, M., Saltbones, J., Slaper, H., Sofiev, M., Syrakov, D., Sørensen, J., der Auwera, L., Valkama, I., Zelazny, R.*, 2004: Ensemble dispersion forecasting – Part I: concept, approach and indicators. *Atmos. Env. 38(28)*, 4607-4617.

Haszpra, T., Lagzi, I., and *Tél, T.*, 2013: Dispersion of aerosol particles in the free atmosphere using ensemble forecasts. *Nonlinear Proc. Geoph. 20*, 759–770.

Haszpra, T. and *Tél, T.*, 2013: Escape rate: a Lagrangian measure of particle deposition from the atmosphere. *Nonlinear Proc. Geoph. 20*, 867–881.

Holt, T., Pullen, J. and *Bishop, C.H.*, 2009: Urban and ocean ensembles for improved meteorological and dispersion modelling of the coastal zone. *Tellus A 61*, 232–249.

Lee, J.A., Peltier, L.J., Haupt, S.E., Wyngaard, J.C., Stauffner, D.R., and Deng, A., 2009: Improving SCIPUFF dispersion forecasts with NWP ensembles. *J. Appl. Meteorol. Climatol. 48*, 2305–2319.

Leutbecher, M. and *Palmer, T.N.*, 2008: Ensemble forecasting. *J. Comput. Phys. 227*, 3515–3539.

Molteni, F., Buizza, R., Palmer, T.N., and *Petroliagis, T.*, 1996: The ECMWF ensemble prediction system: Methodology and validation. *Q. J. Roy. Meteor. Soc. 122*, 73–119.

Scheele, M.P. and *Siegmund, P.C.*, 2001: Estimating errors in trajectory forecasts using ensemble predictions. *J. Appl. Meteorol. 40*, 1223–1232.

Straume, A.G., 2001: A more extensive investigation of the use of ensemble forecasts for dispersion model evaluation *J. Appl. Meteorol. 40*, 425–445.

Straume, A.G., Koffi, E.N.D. and *Nodop, K.*, 1998: Dispersion modeling using ensemble forecasts compared to ETEX measurements. *J. Appl. Meteorol. 37*, 1444–1456.